

Design and Modeling of a Planar Micro-Coil for Micro Solar Converter Application

Abstract. This paper presents a method of dimensioning a DC-DC micro-converter connected to a photovoltaic generator. We are interested in designing and dimensioning a circular planar micro-coil integrated into a Boost micro-converter in this work. The integration of the active and passive power components and the miniaturization of these structures allow a maximum reduction of the space requirement while guaranteeing an acceptable efficiency and improvement of the energy conversion systems' characteristics. The chosen compact model's electrical and frequency behavior, containing all the integrated inductance technological parameters, is described by analytical expressions whose resolution is made using simulation software.

Streszczenie. Przedstawiono metodę projektowania mikrocewki przekształtnika DC-DC podłączonego do ogniwa fotowoltaicznego. Projektowano cewkę okrągłą scaloną z przekształtnikiem typu Boost. Celem była maksymalna miniaturyzacja ale nie kosztem parametrów układu. (Projekt planarnej mikrocewki do przekształtnika typu Boost)

Keywords: Integrated, Micro-coil, DC-DC Micro-Converter, Photovoltaic generator.

Słowa kluczowe: mikrocewka planarna, przekształtnik typu Bpoost

Introduction

For many years, the world of power electronics has been racing in the growing direction of miniaturization and electronic circuits' integration. This miniaturization has pushed towards developing distributed architectures and embedded systems on System-on-chip, containing several components.

The reduction in the size and volumes of more advanced electronic components makes it possible to board more and more functions in the equipment and accessories portable consumer, such as MP4 players, cameras,... These the last ones become multifunctional [1,2]. This increase in the number of functions such as data transmissions, image capture, and processing, speech recognition, is now accompanied by a great need for miniaturized and efficient energy sources.

Today, studies conducted on the optimization of static energy converters, which rely on passive components, can be generalized to many applications concerning their power supply [3]. The aims are to minimize size and volume while maintaining performance and limiting development costs for new products. Looking at my old calculator, I imagine my phone or tablet placed on the table and charge automatically without a charger. For this, the fact that research evolves towards developing renewable energies, we considered it useful to integrate an electric energy converter in a conversion system, which will essentially allow the use of these structures in embedded systems weak power.

Two criteria will guide the sizing of the integrated coils constituting the micro converters. The first is the geometric form or topology of the structure; the second is related to the nature of the materials used to manufacture different parts. These two criteria will affect the value of inductance, stored energy, and losses in the core and the conductor.

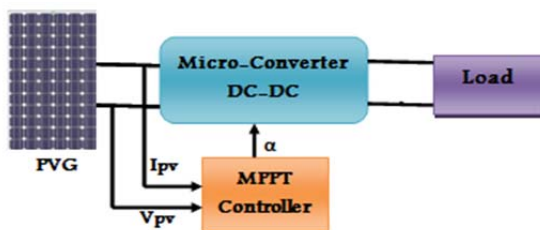


Fig.1. Solar energy conversion system by a DC-DC Boost micro-converter

The topology of the integrated coil that we studied is of a circular planar shape, to integrate it into a DC-DC micro-converter of the Boost type. Generally, the Boost converter's power supply comes from a generator or another DC source. The new in this paper, we combined a micro converter with a free source like a photovoltaic generator (PVG) of power 3W (figure 1).

Dimensioning of the micro-converter

The micro converter is the starting point of the design of the micro-coil. We have chosen a voltage-boosting DC / DC boost micro converter, it is composed of a coil and few passive components, and its electric circuit is represented in figure 2 [3,4]:

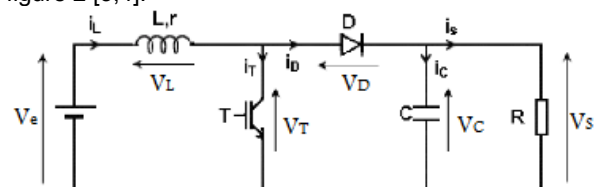


Fig. 2. Structure of the Boost micro converter.

To evaluate this case concretely, we choose the following specifications:

- Input voltage: $V_e = 3$ Volts
- Output voltage: $V_s = 5$ volts
- Output power: $P_s = 3$ W
- Operation frequency: $f = 500$ kHz

According to the structure and specifications of the Boost micro-converter, we deduce the electrical characteristics using the following relations [5]:

Duty cyclic :

$$(1) \quad \alpha = 1 - \frac{V_e}{V_s}$$

At the time $t = \alpha T$ the current $I_L(t)$ in the inductance reaches its peak value, then:

$$(2) \quad I_L(\alpha T) = I_{\max} = \frac{V_e}{V_s} \cdot \alpha T + I_{L\min}$$

From the relation (2), an expression of the undulation $I_L(t)$ is deduced :

$$(3) \quad \Delta I_L = I_{Lmax} - I_{Lmin} = \frac{V_e}{V_s} \cdot \alpha T$$

Considering a lossless circuit, the source's average power P_e is equal to the average power available at the output P_s . The expressions of P_e and P_s are respectively as follows:

$$(4) \quad P_e = V_e I_e$$

$$(5) \quad P_s = V_s I_s$$

The average output power and voltage allow us to calculate the average output current.

$$(6) \quad I_{savg} = \frac{P_{savg}}{V_{savg}}$$

We have :

$$(7) \quad I_{savg} = I_{Lavg} - I_{cavg}$$

$I_{cavg} = 0$ since the average current passing through the capacitor is zero in steady-state.

$$(8) \quad I_{Lavg} = I_{savg}$$

For the critical conduction mode:

$$(9) \quad (\Delta I_L)_{max} = I_{Lmax} - I_{Lmin}$$

With $I_{Lmin} = 0$ (critical conduction mode)

$$(10) \quad (\Delta I_L)_{max} = I_{Lmax} = 2I_{Lavg}$$

From the expression (3), we can calculate the value of the inductance of our coil :

$$(11) \quad L = \frac{\alpha V_e}{(\Delta I_L)_{max} f}$$

The capacity of the Boost converter is given by the following formula (12). For a voltage undulation less than 0,1V, the capacitor C is equal to:

$$(12) \quad C = \frac{\alpha I_s}{\Delta V_s f}$$

The load resistance of the boost converter is:

$$(13) \quad R = \frac{V_s}{I_s}$$

The total magnetic energy stored:

$$(14) \quad W = \frac{1}{2} L I_{Lmax}^2$$

Table 1 summarizes the electrical parameters of Boost micro converter:

Table 1. Electrical parameters of Boost micro converter

Parameter	Symbol	Value
Duty cyclic	α	0,4
The inductance of the coil	L (μ H)	2
Load resistance	R (Ω)	8.33
Capacity	C (μ F)	9,6
Magnetic energy stored	W (μ J)	1.44

Dimensioning of the micro-coil

The spiral planar coil is geometrically described by seven parameters as shown in figure 3: The width of the

conductor w , its thickness t , the spacing between the turns s , the total length of the conductor l_t , also the number of turns n ; its outer diameter D_{out} and inner D_{int} , must be chosen to optimize the ratio between the inductance value and the area occupied on the circuit [3,4].

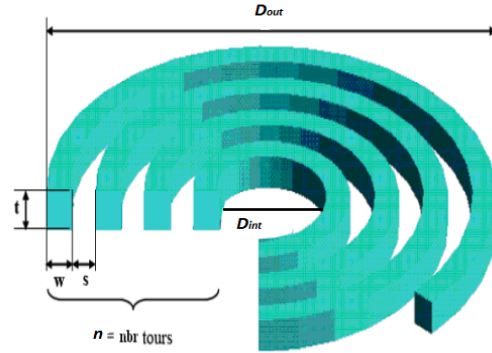


Fig. 3. Geometric parameters of an inductor planar spiral Based on the Mohan [6] method giving the expression of the inductance of a planar coil

$$(15) \quad L \cong \frac{\mu n^2 D_{avg} c_1}{2} \left(\ln\left(\frac{c_2}{\rho}\right) + c_3 \rho + c_4 \rho^2 \right)$$

The coefficients c_1 , c_2 , c_3 and c_4 depend on geometrical form used. For the circular geometry [6]:

$$c_1 = 1, \quad c_2 = 2,46, \quad c_3 = 0, \quad c_4 = 0,2.$$

So, we deduce the number of turn n from the following relation:

$$(16) \quad n = \sqrt{\frac{2L}{\left(\mu_0 \mu_r D_{avg} c_1 \right) \left(\ln\left(\frac{c_2}{\rho}\right) + c_3 \rho + c_4 \rho^2 \right)}}$$

with, $\mu = \mu_0$: for inductances without magnetic core, and $\mu = \mu_0 \mu_r$ for inductors with magnetic core.

The next ties define the form factor and the mean diameter:

$$(17) \quad \rho = \frac{D_{out} - D_{int}}{D_{out} + D_{int}}$$

$$(18) \quad D_{avg} = \frac{D_{out} + D_{int}}{2}$$

The average length of the conductor in a circular planar inductor is determined from the expression(19):

$$(19) \quad l_t = n\pi D_{avg}$$

The calculation of the thickness t and the width w of the winding conductor depends on skin thickness (equation 20), which determines the width of the zone where the current concentrates in a conductor [7, 8]:

$$(20) \quad \delta = \sqrt{\frac{\rho}{\pi \mu f}}$$

To avoid the problem of the skin effect and make the current flowing in the entire conductor, it is necessary to fulfill one of the following conditions [6]:

$$(21) \quad w \leq 2\delta \text{ or } t \leq 2\delta$$

For a rectilinear conductor, the current density for x ranging from 0 to $t/2$ is given by [7,8]

$$(22) \quad j(x) = j_0 e^{-\frac{x}{\delta}}$$

So, the average value of current density is:

$$(23) \quad J_{avg} = \frac{j_0 \left(e^{-\left(\frac{t}{2\delta}\right)} + 1 \right)}{2}$$

One parameter, the thickness t or the width, w is set to find the other. We set the thickness of the conductor $t = 80 \mu\text{m}$; the width is derived from equations (24) and (25).

$$(24) \quad J_{avg} = \frac{I}{S_c}$$

$$(25) \quad S_c = wt$$

In most cases, the micro coils are in contact with the substrate with good conduction properties of temperature. This allows us to use the boundaries conditions: $j_0 = 10^9 \text{ A/m}^2$.

The spacing between windings s can be easily deduced from the geometrical form used:

$$(26) \quad s = \frac{D_{out} - D_{int} - 2nw}{2(n-1)}$$

We set the outer diameter: $D_{out} = 15 \text{ mm}$ and the inner diameter of the coil: $D_{int} = 3 \text{ mm}$.

For coil winding, copper is the optimal material in terms of resistivity, deposit, and cost. Its resistivity is equal to $\rho_{cu} = 1.7 \mu\Omega \cdot \text{cm}$ [8]. We choose the NiFe alloy for the magnetic core, and its relative magnetic permeability is $\mu_r = 800$ and maximum induction of saturation: $B_{max} = 600 \text{ mT}$. [9]

After calculations, we obtain the values of the dimensions of the micro-coil, summarized in the following table:

Table 2. The geometric parameters of the inductor

Geometrical parameters	Dimensioning results
Turn number: n	16
Average length: l_t	45.2 cm
Conductor width: w	18 μm
Conductor thickness: t	80 μm
spacing between windings : s	380 μm

Electrical micro-coil parameters

From the physical model of Yue and Yong [10], we can deduce the equivalent electric circuit of a spiral planar inductance integrated on silicon .reflecting the proximity effects, the parasitic effects, and the frequency effects:

According to the π assembly of the integrated coil figure.4, we deduce the electrical micro-coil parameters using the following relations [10,11]:

Serial resistance (DC) of the winding:

$$(27) \quad R_s = \frac{\rho_{cu} l_t}{wt}$$

Coupling capacitance of the winding:

$$(28) \quad C_s = t l_t \frac{\epsilon_0}{s}$$

The resistance of the silicon substrate:

$$(29) \quad R_{sub} = \rho_{si} \frac{h}{l_t w}$$

With:

$$(30) \quad R_{sub1} = R_{sub2} = 2R_{sub}$$

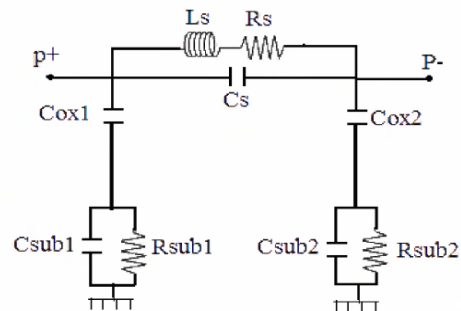


Fig 4. Electrical circuit equivalent in $\llcorner\pi\gg$ of a spiral planar inductance.

The capacitance associated with the silicon substrate:

$$(31) \quad C_{sub} = \epsilon_0 \cdot \epsilon_r \frac{l_t w}{h}$$

With:

$$(32) \quad C_{sub1} = C_{sub2} = \frac{C_{sub}}{2}$$

We set the thickness of the selected substrate: $h = 14 \mu\text{m}$. Oxide capacitance :

$$(33) \quad C_{ox} = \frac{1}{2} l_t w \cdot \frac{\epsilon_0 \cdot \epsilon_{ox}}{t_{ox}}$$

The oxide material used is the Silicon dioxide (SiO_2) its relative permittivity $\epsilon_r = 3.9$

The values of the electric parameters of the integrated on silicon substrate are grouped in the following table:

Table 3. The electric parameters of integrating coil

Electric parameters	Dimensioning results
Inductance: L	2 μH
Coil resistance: R_s	7.96 Ω
Coupling capacitance: C_s	0.84 pF
Substrat resistance : R_{sub}	344 n Ω
Substrat capacitance: C_{sub}	30.6 pF
Oxyde capacitance: C_{ox}	14.04 pF

Technical characteristics of the used solar panel

The photovoltaic generator (PVG) is responsible for the conversion of solar energy into electrical energy. Because this study aims to minimize size and volume while maintaining performance, it was necessary to use a smaller solar panel with real features, as shown in table 4.

Table 4. Technical characteristics of solar panel

Maximum power $P_{max}(w)$	3
Open circuit voltage	3.601
Voltage for maximum	3
Current for maximum power	1
Short circuit current	1.08
Temperature coefficient $V_{oc}(\% \text{ deg.c})$	-0.37201
Temperature coefficient $I_{sc}(\% \text{ deg.c})$	0.058995

Simulation of the electric model of the photovoltaic system

The circuit of figure 5 shows the simulation of a photovoltaic system with a micro converter containing a simple coil, while the circuit of figure 6 shows the

simulation of a photovoltaic system with a micro converter comprising the electrical circuit of integrated inductance model (figure 4):

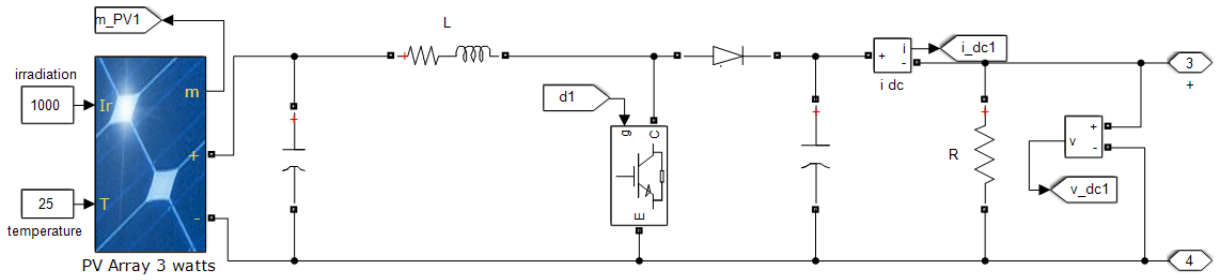


Fig. 5. Photovoltaic system + MPPT and micro converter with a simple coil

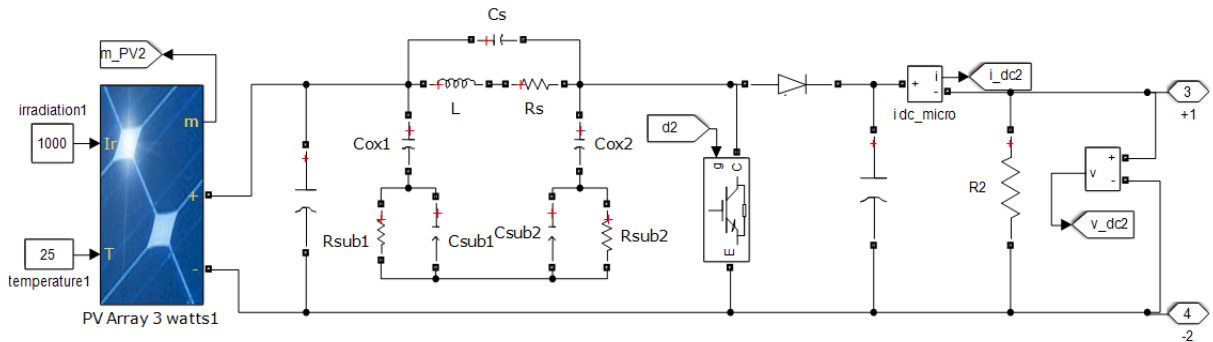


Fig. 6. Photovoltaic system + MPPT and micro converter with an integrated inductance.

After simulation of the two electric circuits, we obtain the principal quantities variations, shown in figures (7,8).

and the frequency effect, where we have considered here just the DC resistance.

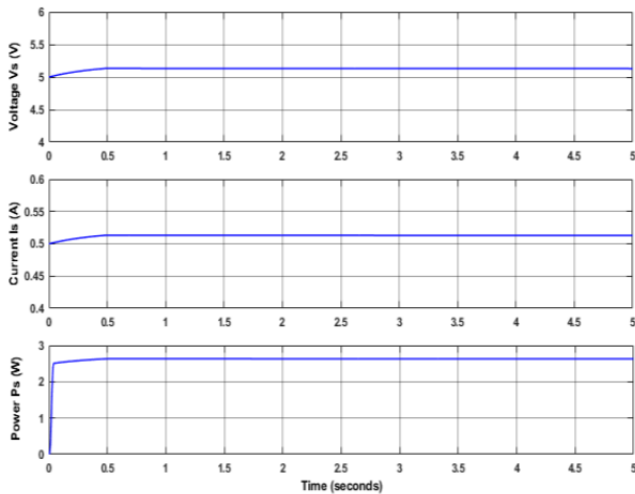


Fig 7. Results of the simulation of the photovoltaic system with a simple coil.

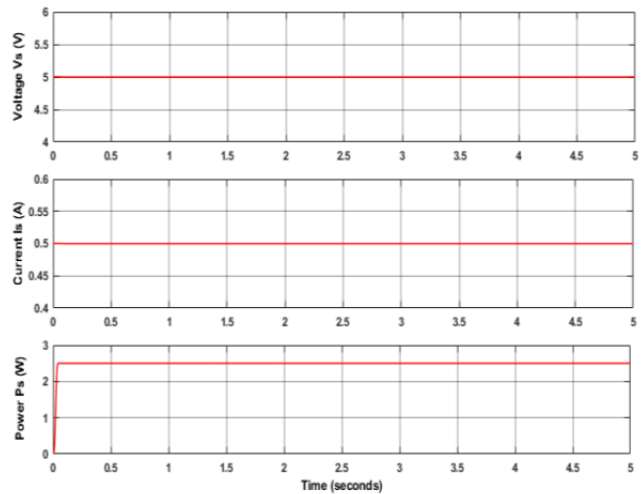


Fig 8. Results of the simulation of the photovoltaic system with an integrated inductance.

The curves of figures (7,8) show the transient and steady-state of the micro converter's electrical behavior. For a real coil, the output voltage is 5.12 V, and the output current equal to 0.52 A, while micro converter simulation with an integrated coil gives an output voltage 4.99 V and an output current similar to 0.5 A. In a steady state, the output power is 2.6 W instead of 3 W. These values (output Voltage, current, and power) are close to the ordered values (5V, 0.6A, 3W). The slight difference is due to the voltage drop across diode and transistor, the resistive losses in the conductor and then, the magnetic core losses,

The efficiency found is around 84%, so near to an operating Boost converter's performance, which is 86%. We conclude that this reduction corresponds to the joules losses generated by conducting windings and the iron losses in the magnetic core.

Influence of the frequency on the value of the inductance and the series resistance

We notice that the inductance decreases in a hyperbolic way when the frequency increases. At low frequencies, the inductance reaches its maximum because the series

resistance is low. As the frequency increases, more and more, the combined effect of the skin effect and the inter-turn capacity degrades the inductance.

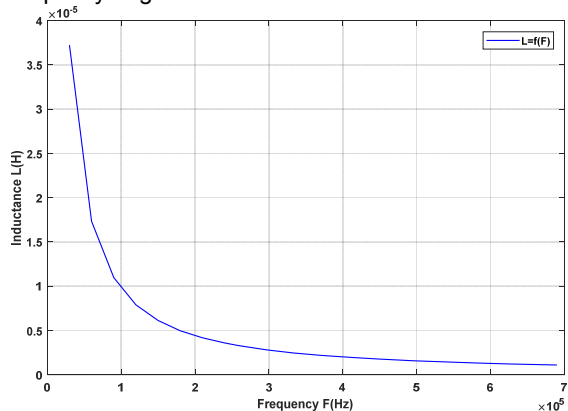


Fig 9. Variation of inductance as a function of frequency $L = f(F)$

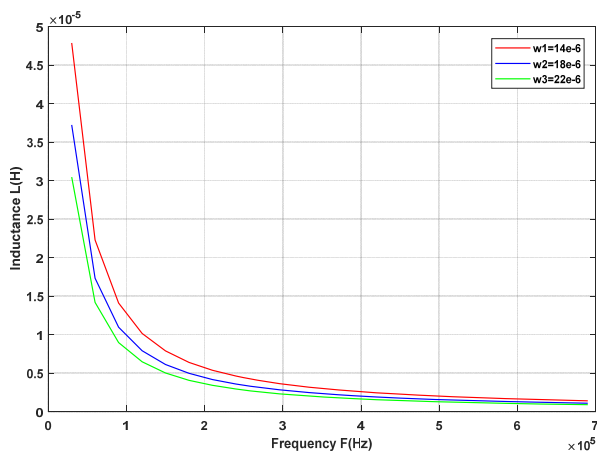


Fig 10. Variation of inductance as a function of frequency for different values of the width of the conductor.

Analysis of the figure.10 shows that for a given frequency, the inductance increases when the width of the conductor decreases. The widening w of the conductors (while respecting the condition $w \leq 2\delta$) acts mainly on the series resistance, which reduces, thus causing the increase in the value of the inductance.

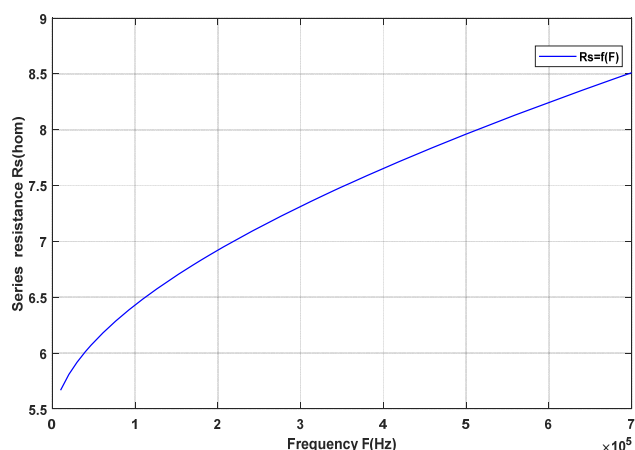


Fig 11. Variation of the series resistance as a function of the operating frequency

When the frequency increases, the skin thickness decreases rapidly, causing the conductor or the current to flow becomes increasingly weak; Consequently, the useful cross-section of the conductor decreases and, consequently, the series resistance increases, leading to significant losses by the Joule effect.

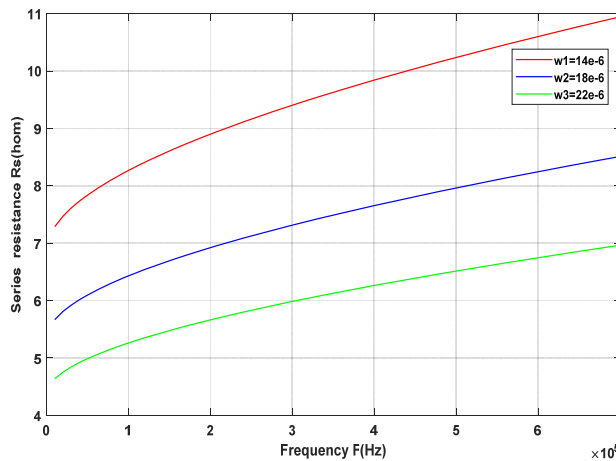


Fig 12. Variation of the series resistance as a function of frequency for different values of width of the conductor.

Figure 12 shows the values of series resistances varying with frequency for different widths of the conductor w . These widths range from 14 μm to 22 μm . The inter-turn space s and the number of turns n are constant. We can deduce that the decrease in the conductors' width as a function of the frequency causes an increase in the series resistance. Also, the reduction in the width of the conductors increases the inductance.

Conclusion

In this paper, we have presented the dimensioning, the modeling, and the simulation of a circular planar micro coil in a micro converter. First, we have determined the electrical parameters of the Boost micro converter according to its specifications. Then, we have calculated the geometrical parameters taking into account the skin effect. We deduced its electric parameters based on the electric circuit model of the integrated planar micro coil on the substrate.

By using a software simulation MATLAB, we compared the converter waveforms, output voltages, output current and output power for the two simulations cases, a micro converter with a classic coil and an integrated planar coil. After the transient state, the output voltage is close to the desired value. This simulation aims to show the performance of an integrated planar micro-coil. To improve these performances, it is necessary to develop the electrical circuit in figure 4, taking into account the electrical characteristics of magnetic material.

Thus, we can conclude that the Boost micro converter containing an integrated coil will essentially allow use in renewable energy conversion systems and low power embedded systems while giving an almost identical performance to those provided by a conventional coil and guaranteeing besides, an integrated compact structure.

Authors:

PhD Student, Abdallah LAIDI,
E-mail: laidi_abdallah@univ-adrar.dz,
Prof. Messaoud HAMOUDA,
E-mail mes.hamouda@univ-adrar.dz,
PhD Student, Mohamed Amine HARTANI,
E-mail: hartani_mohamed@univ-adrar.dz,
Laboratoire de Développement Durable et Informatique (LDDI),
Faculté des Sciences et de la Technologie, Université Ahmed Draïa - Adrar, Algérie.
Dr. Djilalia GUENDOZ, E-mail: lila.guen@yahoo.fr,
Department of Instrumentation maintenance, Oran 2 University, Algeria.

REFERENCES

- [1] Martin C, Allard B., Tournier D., Soueidan M, Rousseau JJ, Allessem D, Menager L, Bley V, Lembeye JY. Planar inductors for high-frequency DC-DC converters using microwave magnetic material. In IEEE 2009 Energy Conversion Congress and Exposition Conference; 20–24 September 2009; San Jose, CA, USA. New York, NY, USA: IEEE. pp. 1890-1894.
- [2] Magali B., Composants passifs intégrés dédiés à la conversion et au stockage de l'énergie. Micro et nanotechnologies/Microélectronique. These Doctorat., (2013), Université Paul Sabatier - Toulouse III.
- [3] Olivier D., Conception, réalisation et mise en œuvre d'un micro-convertisseur intégré pour la conversion DC / DC. (2009), These Doctorat. Université Joseph Fourier.
- [4] Gomes P., Monolithic Power Combiners in n-Chip Spiral Inductors for Silicon-Based Radio-Frequency Integrated Circuits Center. for Integrated Systems Stanford University, CA.
- [5] Ferrieux J. P., Forest F., Alimentations à découpage – Convertisseurs à résonance., (1999), Ed Dunod, 3ème édition.
- [6] Mohan S., The design, modelling and optimization of on-chip inductor and transformer circuit., (1999), Doctoral dissertation, Stanford University.
- [7] C. Patrick Yue., On-Chip Spiral Inductors for Silicon-Based Radio-Frequency Integrated Circuits Center. for Integrated Systems Stanford University, CA.
- [8] Ghannam A., Conception et intégration 'Above IC' d'inductance à fort coefficient de surtension pour application de puissance RF., (2010), Université Toulouse III – Paul Sabatier.
- [9] Roozeboom F., Soft-magnetic fluxguide materials., (1998), Philips Journal of Research N°1.
- [10] Yu Cao., Frequency-Independent Equivalent Circuit Model for On-Chip Spiral Inductors., (2003), IEEE journal of solid-state circuits, (Vol. 38)
- [11] Mayevskiy Y., Analysis and Modeling of Monolithic On-Chip Transformer on silicon Substrates., (2005) Oregon state University, USA.